



Cloning and Characterization New Gly-Asp-Ser-Leu Esterase/Lipase from *Pseudoxanthomonas taiwanensis* AL17

Deviyanthi Nur Afifah,¹ Leyla Novita Brigiyanti,¹ Aulia Qisti,¹ Luxy Grebers Swend Sinaga,¹ Reza Aditama,¹ Made Puspasari Widhiastuty,¹ Elvi Restiawaty² and Akhmaloka^{1,*}

Abstract

A thermostable Gly-Asp-Ser-Leu (GDSL) family esterase encoding gene, namely ITBGDSL_1, was directly cloned from the genomic DNA of *Pseudoxanthomonas taiwanensis* AL17. Homological analysis revealed that the enzyme contained all conserved regions of GDSL family esterase despite a low homology to other GDSL enzymes. Recombinant fusion hexahistidine-tagged ITBGDSL_1 was overexpressed and purified. Biochemical properties were characterised. ITBGDSL_1 having maximal activity to pNP C2. The enzyme was observed to have the highest activity at 55 °C. ITBGDSL_1 exhibited the highest activity at pH 8. Different from other thermostable GDSLs, ITBGDSL_1 showed stability up to 60 h following incubation at optimal temperature. The activity of ITBGDSL_1 preferred more polar solvents and was inhibited by Ethylenediaminetetraacetic acid (EDTA), Phenylmethylsulfonyl fluoride (PMSF), β -mercaptoethanol, and surfactants. Furthermore, the activity was influenced in the presence of metal ions. Monovalent metal ions, such as Na⁺ and K⁺, deactivated the enzyme; meanwhile, most divalent metal ions activated it. Unlike the other GDSL enzymes, the activity was inhibited by the presence of Cu²⁺ or Zn²⁺ ions; the activity of ITBGDSL_1 was increased. This was confirmed by the orientation change at his loop. ITBGDSL_1 is a new member of GDSL family esterase and may employ a distinct catalytic mechanism.

Keywords: Gly-Asp-Ser-Leu; *Pseudoxanthomonas taiwanensis*; Thermostable; Hydrolytic activity.

Received: 20 January 2025; Revised: 22 February 2025; Accepted: 17 March 2025.

Article type: Research article.

1. Introduction

Glycine, Aspartate, Serine, Lysine (GDSL) motif enzyme represents a relatively recent subclass of hydrolytic enzymes that remains incompletely understood.^[1-3] The GDSL was first reported by Upon and Buckley.^[4] Since then, numerous research endeavors have sought to elucidate the functions of these hydrolytic enzymes. The enzymes were isolated from various origins, including plants and microorganisms.^[5-10] Some lipases (EC 3.1.1.3) and esterases (EC 3.1.1.1) contain a GX SXG motif, with the active site serine (S) residue positioned in the middle of the conserved sequence. Nevertheless, it is crucial to note that not all lipolytic enzymes exhibit the common motif. A new subgroup of these

hydrolytic/lipolytic enzymes, formerly known as GDSLs and later called GDSL, presents a distinct motif with the active site serine near the N-terminus.^[11-13] Enzymes belonging to the GDSL esterase/lipase family exhibit five highly conserved homology blocks, critical for their classification.^[14,15] The GDSL esterase/lipase family is categorized as SGNH hydrolase due to the presence of highly conserved residues, namely Ser-Gly-Asn-His, found in blocks I, II, III, and V.^[11-13] GDSL esterase/lipase enzyme plays a crucial role in synthesizing or hydrolysis of compounds containing esters. As part of the GDSL esterase/lipase family, esterases hydrolyze fatty acid esters with acyl chain lengths of less than ten carbon atoms. In the industrial sector, the utilization of GDSL esterase/lipase enzymes was widespread, encompassing food processing, beverages, perfume, chemical, agricultural, and pharmaceutical industries.^[16] Interestingly, some GDSL esterase/lipase families are multifunctional, demonstrating activities such as thioesterase, esterase, arylesterase, protease, and lysophospholipase.^[17] The flexible active site environment within the GDSL esterase/lipase family leads to broad substrate specificity. Previous research highlighted conformational changes as a unique feature of multifunctional

¹ Biochemistry and Biomolecule Engineering Research Group, Faculty of Mathematics and Natural Sciences, Institut Teknologi Bandung, Jl. Ganesha no.10 Bandung, 40132, Indonesia

² Chemical Engineering Process Design and Development Research Group, Faculty of Industrial Technology, Institut Teknologi Bandung, Jl. Ganesha no.10 Bandung, 40132, Indonesia

*Email: loka@itb.ac.id (Akhmaloka)

GDSL enzymes.^[14,15]

In recent years, the utilization of GDSL esterase/lipase enzymes from thermophilic bacteria in industries has been significant.^[18] Several thermostable GDSL esterase/lipase from *Fervidobacterium nodosum*,^[19] *Geobacillus stearothermophilus*,^[2] *Ruminococcaceae bacterium*,^[20] *Geobacillus thermodenitrificans*,^[1] *Bacillus sp.*,^[21,22] *Geobacillus thermocatenulatus*,^[10] *Pseudomonas sp.*,^[23] were characterized and reported. However, these enzymes still need to fully meet the industrial demands for specific properties, prompting further research to discover and characterize new GDSL esterase/lipase enzymes from thermophilic bacteria were needed.

In this study, cloning, expression, and characterization of a new GDSL esterase from *Pseudoxanthomonas taiwanensis* were reported. The enzyme shows low homology with other GDSL enzymes reported, with the highest (37%) to GDSL *Bacillus sp.*, K91.

2. Materials and methods

2.1 Growth condition of AL17

Bacterial culture AL17 was obtained from a collection of thermophilic microorganisms from our laboratory, originally isolated from household compost at the Waste Disposal Site, Saraga, ITB, Bandung.^[24] The glycerol stock of bacteria was incubated at 50 °C overnight. The bacteria were transferred from the liquid to solid media by an aseptic method and incubated at 50 °C for 17 hours. Single colonies of bacteria were transferred with ose to liquid media and incubated overnight at 50 °C.

2.2 Cloning of ITBGDSL_1

ITBGDSL_1 was amplified by PCR from genomic DNA through a pair of primers, namely GDSL_1 forward (ATGCACCGGATCCCCCGC), and GDSL_1 reverse (TCAGTGCGGCCGGGCCG). A 25 µL reaction mixture containing 18.5 µL mix *KOD One*TM - *PCR* Master Mix (TOYOBO), 10 pmol of the forward and reverse primers, and 2 ng of genomic DNA was prepared. PCR was performed under the following conditions: 10 s at 98 °C, 5 s at 65 °C, 10 s at 68 °C for 25 cycles, and 10 min final extension at 68 °C. The PCR fragments were purified from agarose gels using Top Vision Agarose and cloned into pJet1.2/blunt easy vector using The CloneJET PCR Cloning Kit (Thermo ScientificTM). The insert was then sequenced and analyzed.

2.3 Expression and Purification of ITBGDSL_1

To express ITBGDSL_1 into *E. coli* BL21 (DE3), the recombinant expression vector was constructed on pET-30a(+). The target gene was re-PCR using a pair of primers containing *NdeI* and *XhoI* restriction sites with forward primer

namely: GDSL1_Fex (CAACATATGCACCGGA TCCCCCGC), and reverse primer, namely GDSL1_Rex (AGACTCGAGGTGCGGCCGGGCCG). The PCR product was analyzed through agarose gel electrophoresis and purified using GeneJET gel extraction KIT by Thermo ScientificTM. The pET-30a(+) plasmid and the gene fragments were digested with *NdeI* and *XhoI*. The product was ligated using T4 DNA ligase. The recombinant plasmid was confirmed and transformed into competent cells of *E. coli* BL21 (DE3) for gene expression. A single colony of the recombinant BL21 (DE3) was cultivated in LB medium supplemented with 50 µg/mL of kanamycin at 37 °C, until cultures reached an OD 600 of 0.6. The cells were induced with 1 mM isopropyl β-D-1-thiogalactopyranoside (IPTG), and the cultures were incubated with agitation at 37 °C for 4 hours. Subsequently, cells were harvested by centrifugation (at 3000 xg, 4 °C for 30 min), and the resulting pellet was resuspended in 50 mM phosphate buffer (pH 8) containing 0.5% SDS. The cell was lysed by thermolysis at 50 °C for 20 min. The crude cell extracts were centrifuged (at 3000x g, 4 °C for 45 min) to eliminate cellular debris. The supernatant was collected and loaded into Nickel-Nitrilotriacetic acid (Ni-NTA) affinity chromatography column (1 mL; Qiagen, Hilden, Germany). The protein target binds to the resin while other proteins pass through the column. Washing step was performed to remove any remaining contaminants bound to protein using wash buffer. The protein was eluted from the resin using elution buffer containing 100 mM imidazole, 50 mM phosphate buffer (pH 8), and 500 mM NaCl. The molecular weight of the purified enzyme was measured through Sodium Dodecyl-Sulfate Polyacrylamide Gel Electrophoresis (SDS-PAGE).

2.4 Enzyme activity assay

The hydrolytic activity of ITBGDSL_1 was assayed based on a colorimetric technique adapted by Lee *et al.* (1997),^[25] employing the substrate *pNP*-acyl esters. The enzyme-substrate mixture was incubated at 55 °C for 15 min in 50 mM phosphate buffer, pH 8. The enzymatic reaction was terminated through incubation at -20 °C for 10 min. Measurements were performed using UV-Vis spectrophotometry at λ 405 nm. One unit of activity was defined as the quantity of enzyme capable of liberating 1 µL of *pNP* per min under the assay conditions. All experiments were conducted in triplicate. A standard curve was established by measuring the absorbance of solutions containing released *p*-nitrophenol at concentrations ranging from 0 to 10 µg/mL.^[25]

2.5 Variation of substrate

The enzyme substrate specificity was assayed using *pNP*

esters with varying acyl chain lengths ranging from C2 to C18. The reactions were conducted using substrate concentration of 10 mM and standard conditions (50 mM phosphate buffer, pH 8, ethanol 50 mM).

2.6 pH and temperature optimum assay

The effect of pH and temperature was determined using *p*NP-C2 substrate, and incubation at 55 °C for 15 min. Various buffer pHs ranging from 3.0 to 12.0 with a final concentration of 50 mM were used. The buffer of sodium acetate was used for the pH range of 3.0-5.0, sodium phosphate for the pH range at 6.0-8.0, and glycine-NaOH for the pH range at 9.0-12.0. To investigate the effect of temperature on enzyme activity, the assays were performed on variation of temperature range from 30 to 90 °C, with intervals of 5 °C, under optimal pH.

2.7 Thermostability assay

Thermostability was performed by measuring enzyme activity after incubation at 55 °C for various times, from 0 to 60 hours. Enzyme activity was measured under optimum conditions.

2.8 Variation of metal ion

The effect of metal ions on enzyme activity was assayed at optimum conditions. The enzyme was pre-incubated with each selected metal ion at a final concentration of 3 mM at 55 °C for 15 min. The lipolytic activity of the enzyme without metal ion was considered as 100%.

2.9 Variation of surfactants and organic solvents on the activity

The activity of the enzyme against various detergents was also measured by sodium dodecyl sulfate (SDS), Triton X-100, Tween 80, Tween 20, Cetyltrimethylammonium bromide (CTAB), and Tergitol at the final concentration of 3 %. The enzyme was pre-incubated with each detergent under optimal conditions such as temperature, pH, and substrate, for 15 min before activity measurement.

Subsequently, the influence of organic solvents on the activity was also examined. Solvents used ranged from non-polar to polar. Residual activity was measured according to standard conditions. The activity without the addition of detergents was defined as 100%.

2.10 Inhibitor assay

Different inhibitors, including EDTA (3 mM), PMSF (3 mM), and β -mercaptoethanol (3 mM), were added into the reaction mixture consisting of the *p*NP-C2 at pH 8. The enzyme activity was subsequently measured under standard assay at 55 °C. The enzyme without an inhibitor was considered as the

control (100%).

2.11 Computational analysis

Multiple Sequence analysis and constructing phylogenetic tree. Neighbor-Joining program was performed by MEGA11 software.^[26] Secondary structure alignment was carried out using the Promals3D website. The 3D model of ITBGDSL_1 was constructed using the AlphaFold website.^[27] Protein minimization and visualization were carried out using the pyMol software.^[28] Docking analysis was performed using the Autodock Vina.^[29] Hydrophobic clusters, salt bridges, and hydrogen bonds on the protein structure were identified using the ProteinTools server. Analysis of enzyme metal-binding sites was performed using Metal Ion-Binding site prediction and docking server MIB. The catalytic pocket was measured using the CastP website.

3. Results and discussion

3.1 Homology of ITBGDSL_1

ITBGDSL_1 was cloned through *in vitro* amplification by PCR from genomic DNA of AL17, sequenced, and overexpressed in *E. coli* BL21 (DE3). The open reading frame (ORF) contains 1131 base pairs, encoding 376 amino acids. Homological analysis using BLAST revealed that *ITBGDSL_1* was 37.96 % homologous to GDSL of *Bacillus sp.* K91 and 30.81 % to the *Sphingomonas sp.* MJ-3 (Table 1). Phylogenetic tree generated by MEGA-11 software showed that the *ITBGDSL_1* is close to GDSL *Bacillus sp.* K91 (Fig. S1).^[26]

Despite a low homology with other cloned GDSL, the amino acid sequence of *ITBGDSL_1* appears all conserved region of other GDSL (Fig. S2), such as GDS(X) in block I containing serine (S) for triad catalytic, NHAXXG in block II containing asparagine (N) and glycine (G) for oxyanion hole, GHND in block III containing histidine (H) for triad catalytic, and DTTH in block V containing aspartate (D) for triad catalytic. *ITBGDSL_1* lacks an explicit block IV, as other GDSLs are characterised.^[4] The amino acid residues of *ITBGDSL_1* contain an active site (triad catalytic) of Ser-His-Asp preserved in blocks I, III, and V (Fig. S2). The catalysis performed by *ITBGDSL_1* follows the classic mechanism of serine hydrolase hydrolysis.^[4,14] The distinguishing characteristic of GDSL motif is representation as lipolytic enzyme family II, offering several advantages compared to other lipases featuring motifs of lipolytic enzymes such as GX SXG.^[14] The GDSL designates a unique hydrolytic and lipolytic subfamily, displaying different motifs from GX SXG lipase. Notably, serine, as one of the catalytic triad, is located close to the N-terminal region on *ITBGDSL_1* (Fig. S2, Block

Table 1: Homological analysis of enzyme ITBGDSL_1 with other GDSL esterases.

Description	Max Score	Total Score	Query Covert	E Value	Per. Ident	Acc. Len	Accession
GDSL_ <i>Bacillus</i> _sp_K91	147	147	56%	2e-45	37.96%	217	Query_2892640
GDSL_ <i>Sphingomonas</i> _sp_MJ-3	79.0	79.0	50%	9e-20	30.81%	292	Query_2892652
GDSL_ <i>Pseudomonas</i> _sp	29.6	29.6	21%	0.001	24.47%	299	Query_2892655
GDSL_ <i>Anabaena</i> _sp_PCC-7120	25.8	25.8	22%	0.023	26.14%	275	Query_2892656

I) as shown on the other GDSL.^[4] Many studies suggested that the GDSL motif defines a hydrolytic enzyme with multifunctional properties, with broad substrate specificity and regiospecificity. ITBGDSL_1 contains all consensus sequences of GDSL and five pivotal amino acid residues (S, G, N, D, and H) that lie on blocks I, II, III, and V. Ser, Asp, and His form a triad catalytic supported by Gly and Asn as proton donor (Fig. S2). In addition, GDSL hydrolases show a flexible active site, appearing to have conformational changes in response to the presence and binding of different substrates or ligands.^[14]

3.2 3D structure modelling of ITBGDSL_1

The 3D structure modelling of ITBGDSL_1 was constructed by the AlphaFold program using *Lysophospholipase* L1-like esterase (A0A562DZX6.1.A) as template with similarity of 73.33 %.^[27] The structure of ITBGDSL_1 consists of several

domains, including a 4-strand parallel β -sheet, with the addition of two sheets, three inward-curving helices, two outward-curving helices, and short helices (Fig. 1A). The β -sheet is located in the core region surrounded by α -helices to form the typical α/β hydrolase. Three amino acid residues such as Ser10, Asp185, and His188 formed a triad catalytic (Fig. 1A).

Based on protein data bank (PDB), two crystal structures of GDSL were deposited, GDSL from *Photobacterium* sp. and GDSL from *Pseudoalteromonas* sp., namely 5XTU and 3HP4, respectively. The structure of 5XTU contains 4-parallel β -sheet, 5 inward-curving helices, 2 outward-curving helices, and additional short helices (Fig. 1B). Three catalytic residues, Ser12, Asp302, and His305, form a triad catalytic (Fig. 1B).^[30] Meanwhile, the 3D structure of 3HP4 contains a 5-strand parallel β -sheet, 3 inward-curving helices, 2 outward-curving helices, and additional short helices (Fig. 1C). Three

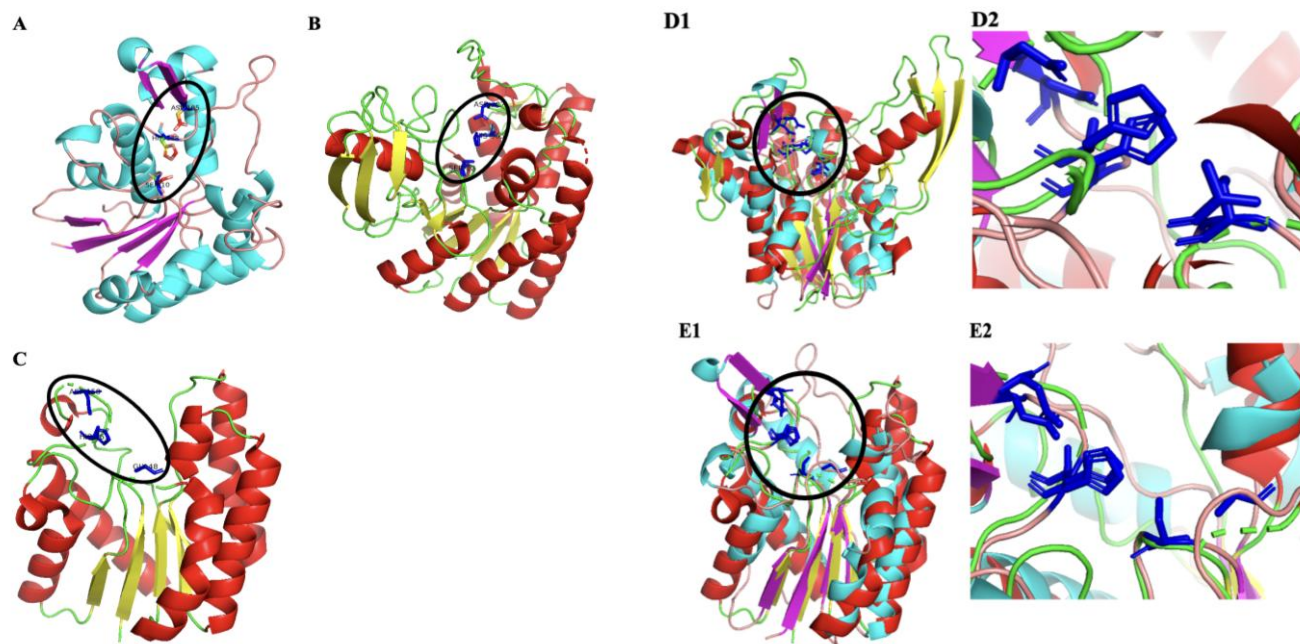


Fig. 1: 3D structure modelling of ITBGDSL_1 with other GDSL lipases using Python Molecular Graphics (PyMol) software. (A) GDSL *P. taiwanensis* (ITBGDSL_1) (this study); (B) GDSL *Photobacterium* sp., (5XTU);^[30] (C) GDSL *Pseudoalteromonas* sp., (3HP4);^[31] (D1) Superimposition between ITBGDSL_1 to 5XTU; (D2) Focusing of triad catalytic; (E1) Superimposition between ITBGDSL_1 to 3HP4; (E2) Focusing of triad catalytic. (○) Orientation of triad catalytic.

Table 2: Hydrolysis activity of ITBGDSL_1. Reaction was performed at 55 °C, pH 8, and para-nitrophenyl acetate (pNP-C2) as substrate.

Enzyme	Unit Activity (U)	Protein Concentration (mg/mL)	Specific Activity (U/mg)	Purification (fold)
Crude extract of ITBGDSL_1	1.490	11.605	0.128	1
Pure enzyme of ITBGDSL_1	2.926	3.468	0.844	6.6

catalytic residues, Gly48, Asp158, and His161, form a triad catalytic.^[31] Superimposition between ITBGDSL_1 to 5XTU and ITBGDSL_1 to 3HP4 showed that there are many differences between the 3D structures of the two entities (Figs. 1D1 and 1E1); however, the conformation of the triad catalytic seems to be conserved (Figs. 1D2 and 1E2). ITBGDSL_1 (46 kDa) exhibits larger size compared to that of *Photobacterium sp.* (5XTU) (36 kDa) and *Pseudoalteromonas sp.* (3HP4) (23 kDa).^[30,31] In addition, the GDSL from *Photobacterium sp.* and the *Pseudoalteromonas sp.* do not show as thermozyms.

3.3 Activity and substrate preference of ITBGDSL_1

ITBGDSL_1 was expressed in *E. coli* BL21 (DE3) following induction of IPTG 1 mM. The cells were disrupted by thermolysis at 50 °C. The crude extract still showed hydrolytic activity (Table 2). The enzyme was purified by IMAC Ni-NTA and exhibited a single band with a molecular weight of approximately 46 kDa (Fig. 2). The purified enzyme showed 6.6 times activity compared to that of the crude extract.

Lipase/esterase shows a preference for specific substrate, especially for carbon chain length or double bonds.^[32,33] The substrate preference of ITBGDSL_1 was determined on varying carbon length from C2-C18. The result showed that ITBGDSL_1 prefers short-chain substrate with the highest on pNP-C2 (Fig. 3). The result suggested that ITBGDSL_1 is an esterase-type enzyme. A few reports of thermostable GDSL are esterases, such as GDSL from *Fervidobacterium nodosum* Rt17-B1 and *Bacillus sp.* K91, both enzymes exhibit optimal activity on the pNP-C2 substrate.^[19,22] However, GDSL from *G. thermodenitrificans* was reported to prefer pNP-C4 as substrate.^[1]

To probe more details on the molecular interaction of ITBGDSL_1, silico analysis was performed. Binding energy of the substrate to the enzyme showed that the affinity energy tends to decrease by shorter carbon chains (Table 3). This suggested that shorter carbon chain substrates are better able to interact with the enzyme, thus increasing the activity. The data is in agreement to the experiment showing the enzyme preferred a short carbon chain substrate (Fig. 3).

Further analysis on molecular docking is to measure the

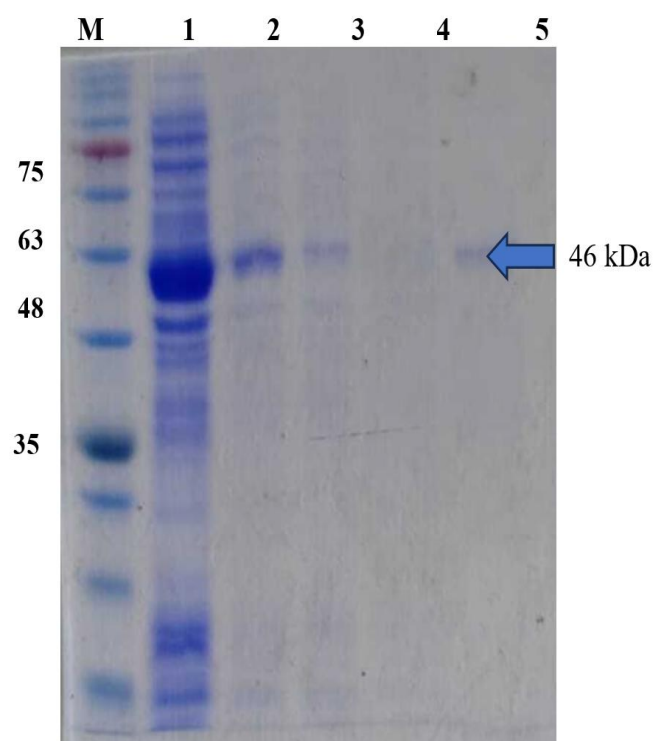


Fig. 2: SDS-PAGE of crude extract and purified ITBGDSL_1. M = marker; (1) total protein; (2) crude extract; (3) flow-through; (4) wash buffer; (5) 100 mM imidazole elution.

distance between the substrate and Ser10 residue, one of the triad catalytic. The result showed that shorter carbon chain substrates tend closer to Ser10 residue (Table 3). A closer orientation of the substrate to the catalytic pocket may lead to better interaction and enhance the activity of the enzyme.^[34] This suggested that C2 substrate is the most preferable substrate for the enzyme. In addition, the catalytic pocket of ITBGDSL_1 revealed smaller compared to that of 5XTU or GDSL from *G. thermocatenulatus* (Table 4). The three enzymes contain the same catalytic triad residues; however, the conformation of catalytic pockets is slightly different. Previous study showed that the orientation difference in the catalytic pocket may lead to a difference in substrate specificity.^[35] 5XTU cavity binding pocket is larger compared to that of ITBGDSL_1 and hence prefers C4 substrate.^[30,31]

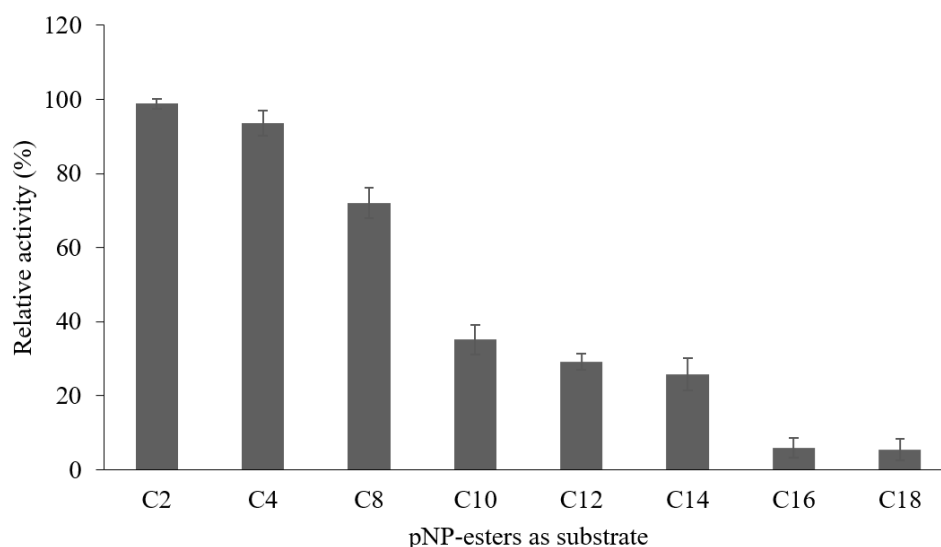


Fig. 3: Hydrolytic activity of ITBGDSL_1 toward different carbon ranges of para-nitrophenyl esters substrate (pNP-esters). para-nitrophenyl acetate (pNP-C2); para-nitrophenyl butyrate (pNP-C4); para-nitrophenyl octanoate (pNP-C8); para-nitrophenyl caproate (pNP-C10); para-nitrophenyl laurate (pNP-C12); para-nitrophenyl myristate (pNP-C14); para-nitrophenyl palmitate (pNP-C16); para-nitrophenyl stearate (pNP-C18).

Table 3: Affinity binding of ITBGDSL_1 and Ser10 - substrate distance. pNP-C2 used as substrate, the distance was measured by Protein-Ligand Interaction Profiler programme (PLIP).

Substrate	Binding Energy (kcal/mol)	Ser10 – Sub (Å)
C2	-4.8	4.1
C4	-4.8	4.2
C8	-4.4	4.7
C10	-4.0	8.5
C12	-3.0	7.8
C14	1.0	9.9
C16	0	10.1
C18	10	9.8

Table 4: Binding pocket volume of ITBGDSL_1 and other GDSL and the substrate preference. The volume was calculated by Computed Atlas of Surface Topography of Proteins programme (CastP).

Enzyme	Volume (Å ³)	Substrate	Reference
ITBGDSL_1	8.874	C2	This study
GDSL <i>Photobacterium sp.</i> , (5XTU)	63.603	C4	[30]
GDSL <i>M. thermotolerans</i> (MT6)	89.129	C10	[36]

Meanwhile, GDSL from *Marinactinospora thermotolerans* showed a cavity binding pocket larger compared to that of ITBGDSL_1 and hence prefers C10 substrates.^[36]

3.4 The effect of temperature and pH on the activity of ITBGDSL_1
Determination of optimal temperature and pH was performed

on the purified ITBGDSL_1 using *p*NP-C2 as substrate. The optimal temperature was assayed, at a temperature range from 30 °C to 90 °C. The activity was assayed based on hydrolysis activity of the enzyme on *p*NP-C2 substrate. The result showed that the activity of the enzyme was increased by increasing temperature from 30 to 55 °C. Further elevating temperature appeared to decrease the activity. At 60 °C, the activity remains 70 % compared to the optimum temperature. Further elevation of temperature showed that the activity of the enzyme was 40 % from its optimal condition at 70 °C (Fig. 4A). Some of the GDSL from *Geobacillus sp.* were reported to exhibit optimum temperature at 55 °C, such as GDSL from *G. thermodenitrificans* and *G. thermocatenulatus*.^[1,10]

The activity of the enzyme is also influenced by the pH condition to maintain hydrogen interactions on the protein conformation. pH influence on protonations and

deprotonations of amino acid residues, thereby affecting its activity.^[37] The optimum pH of ITBGDSL_1 appeared at pH 8 (Fig. 4B). ITBGDSL_1 showed highest homology to GDSL from *Bacillus sp.*^[21] The enzyme also exhibited optimum activity at pH 8. Some of GDSL from *G. thermodenitrificans* and *Ruminococcaceae bacterium* exhibited optimum activity at pH 9. From all of the above data, ITBGDSL_1 is classified as a thermostable and slightly alkaline enzyme.^[1,20]

3.5 Thermostability of ITBGDSL_1

Thermostability is an essential character of the enzyme for industrial applications.^[38,39] Thermostability of ITBGDSL_1 was assayed by incubating the enzyme at optimum temperature for durations of 0 to 60 h. Following incubation, the hydrolysis activity was measured at optimum conditions, 55 °C, pH 8, and *p*NP-C2 as substrate. The result showed that

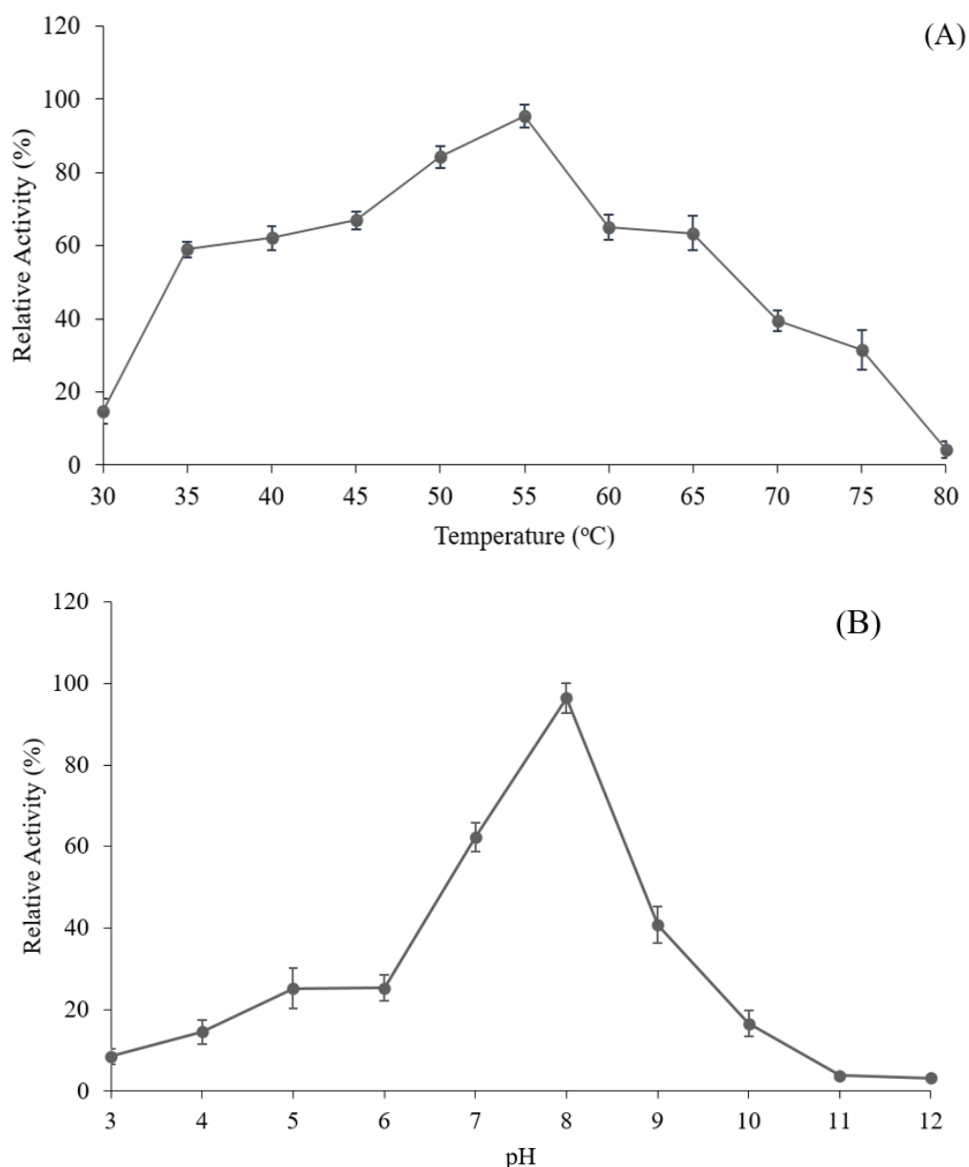


Fig. 4: Relative activity of ITBGDSL_1 in variation of temperature (A) and pH (B). Optimal condition at 55 °C and pH 8.

the residual activity remained at 90 %, after 24 h incubation. The residual activity was retained up to 80 % for 60 h incubation (Fig. 5). The result was surprising since most of GDSL from *Geobacillus sp.*,^[1,10] *F. nodosum*,^[19] *R. bacterium*,^[20] and *Pseudomonas sp.* exhibited thermal stability at its optimal temperature for only 1 – 12 h, and residual activity less than 90 % (Table 5).^[23] Several factors contribute to thermal stability of enzyme, such as hydrogen bonds, hydrophobic interactions, and salt bridges within the protein structure.^[40]

To probe more detail on intramolecular interaction of the enzyme, molecular dynamic simulation was performed on ITBGDSL_1 and compared to TesA, thermolabile GDSL from *Pseudomonas aeruginosa*.^[41] The results showed that Solvent Accessible Surface Area (SASA) was relatively constant during 100 ns simulation at 300 K and 400 K; however, at 500 K, the SASA appeared slightly higher and fluctuated during the simulation (Fig. 6). Comparison of SASA value at 500 K between ITBGDSL_1 and TesA showed that ITBGDSL_1 exhibited lower SASA values compared to TesA (Fig. 6, green line). Indicating that ITBGDSL_1 maintains a more conformationally stable state at higher temperatures. Further analysis on the structure of the protein revealed that the hydrogen bonds were essential for the thermal stability of the protein (Fig. 7). The hydrogen bonds of Asp70-Arg3, Phe76-Tyr96, and Arg102-Thr106 consistently occurred during approximately 60 % of simulation time (Table 6). These interactions were likely stabilized critical regions of ITBGDSL_1, potentially preventing excessive structural rearrangement or unfolding of the protein at high temperatures; hence, ITBGDSL_1 is a highly thermostable protein.

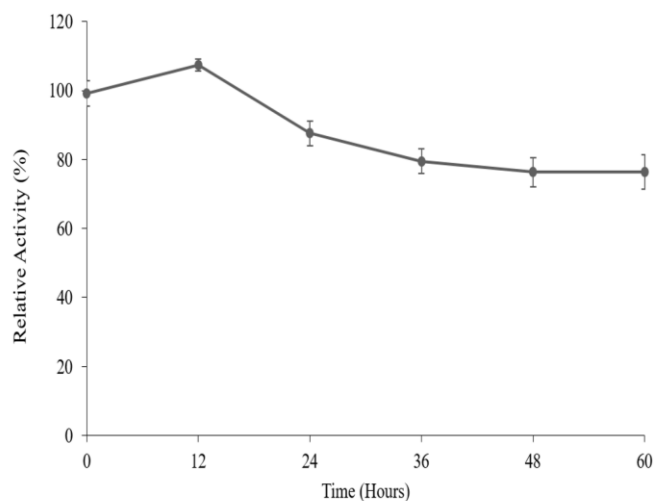


Fig. 5: Residual Activity of ITBGDSL_1 following incubation time at optimal temperature.

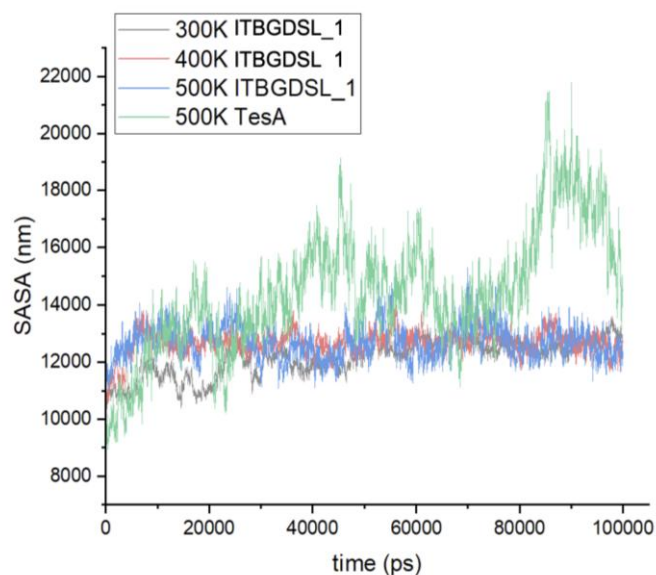


Fig. 6: SASA of ITBGDSL_1 and TesA, generated by Groningen Machine for Chemical Simulation (GROMACS) programme. (black line) ITBGDSL_1 at 300 K; (red line) ITBGDSL_1 at 400 K; (blue line) ITBGDSL_1 at 500 K; (green line) TesA at 500 K.

3.6 The effect of reagent and chemicals on activity of ITBGDSL_1

The activity of ITBGDSL_1 was decreased by decreasing polarity of the solvent with exception of DMSO (Fig. 8). The chemical might interact to the enzyme and inhibit the catalytic reaction. Replacement of ethanol by n-hexane reduced to activity up to 93 %. The data are in agreement with previous reports, such as GDSL from *Bacillus sp.*, which was decreased in the presence of n-hexane.^[21] Meanwhile, GDSL from *G. thermodenitrificans* and *Thauera sp.* were deactivated on methanol as solvent. The data suggested that ITBGDSL_1 prefers more polar solvents.^[1,42]

The activity of ITBGDSL_1 was deactivated by the presence of surfactant (Fig. 9). CTAB was the most reactive detergent to deactivate ITBGDSL_1. The activity of most GDSLs was decreased in the presence of surfactant.^[1,21] EDTA, PMSF, and β -mercaptoethanol inhibited the activity of ITBGDSL_1 (Fig. 10). EDTA is known as a chelating agent and interacts with divalent metal ions. Deactivation of the enzyme in the presence of EDTA suggests that the activity of the enzyme was influenced by divalent metal ions or that the enzyme was classified as a metalloenzyme. PMSF might interact with Serine or Histidine. Deactivation of ITBGDSL_1 in the presence of PMSF suggested that Serine and Histidine residues may be involved in the catalytic mechanism.

3.7 The effect of metal ion on the activity of ITBGDSL_1

Most of the confirmation and activity of the enzymes are

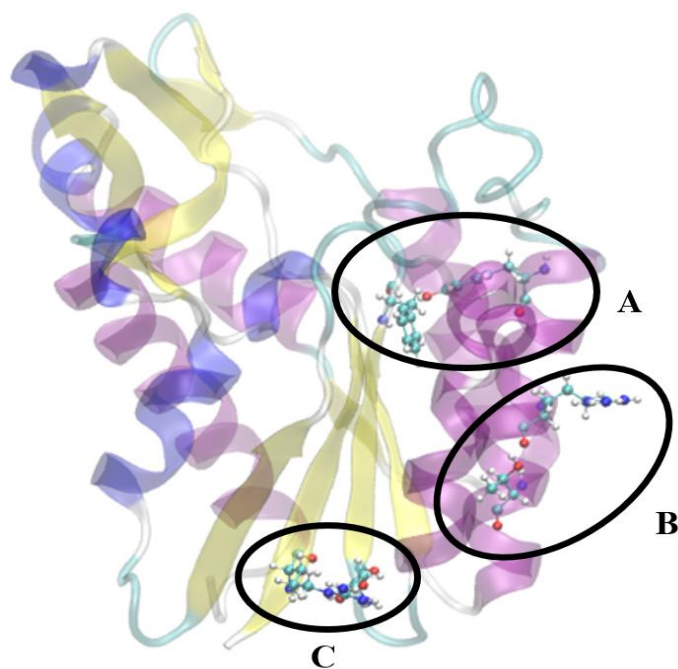


Fig. 7: 3D structure of ITBGDSL_1 with essential hydrogen bonds (○). Three hydrogen bonds between (A) Asp70-Arg3; (B) Phe76-Tyr96; and (C) Arg102-Thr106.

Table 5: Thermostability of ITBGDSL_1 and other GDSL.

No.	Enzyme	Optimum Temperature (°C)	Thermostability (Hours)	Residual Activity (%)	Reference
1	ITBGDSL_1	55	60	80	This study
2	GDSL <i>G. thermodenitrificans</i>	60	12	60	[1]
3	GDSL <i>G. thermocatenuatus</i>	55	3	50	[10]
4	GDSL <i>F. nodosum</i>	75	1.2	40	[19]
5	GDSL <i>R. bacterium</i>	60	1	70	[20]
6	GDSL <i>Pseudomonas sp.</i>	60	3	90	[23]

Table 6: The hydrogen bond of Asp70-Arg3, Phe76-Tyr96, and Arg102-Thr106 on ITBGDSL_1.

Receptor	Donor	Fraction			Distance (Å)		
		300 K	400 K	500 K	300 K	400 K	500 K
Asp70-OD2	Arg3-NH2	0.990	0.766	0.601	2.73	2.74	2.75
Phe76-O	Tyr96-OH	0.953	0.917	0.812	2.69	2.70	2.72
Arg102-O	Thr106-OG1	0.894	0.816	0.661	2.74	2.75	2.75

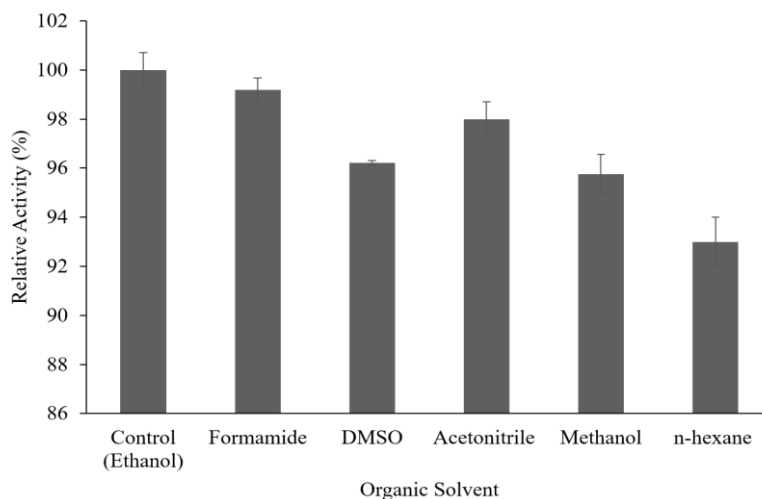


Fig. 8: Relative Activity of ITBGDSL_1 at variation of organic solvent 3 % concentration.

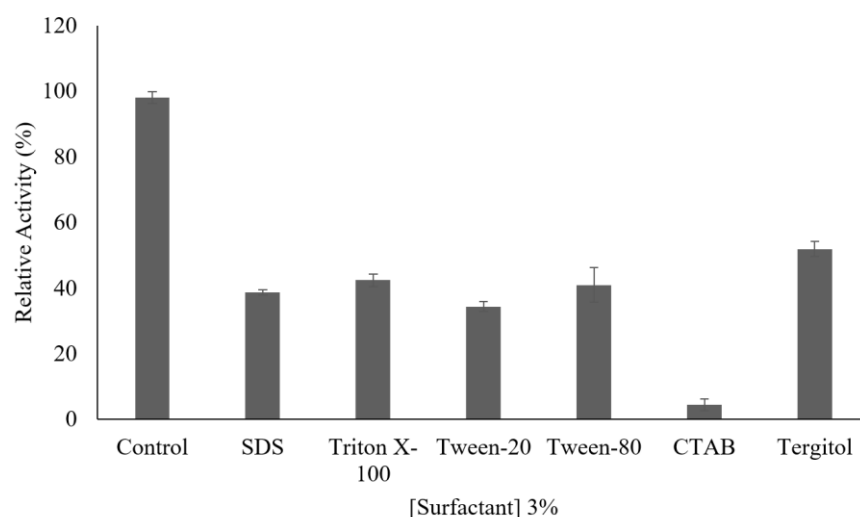


Fig. 9: Relative Activity of ITBGDSL_1 on the present of variation surfactant at 3 % concentration. (Control) Ethanol.

influenced by the presence of metal ions. The effect of metal ions on the activity of ITBGDSL_1 was determined by addition of the metal to the reaction mixture. The activity of ITBGDSL_1 was inhibited by the presence of monovalent metal ions such as Na^+ and K^+ . Meanwhile in the present of divalent metal ions such as Mg^{2+} , Co^{2+} , Ca^{2+} , Mn^{2+} , Ba^{2+} , Mn^{2+} , Fe^{3+} , Cu^{2+} and Zn^{2+} , the activity was increased with the exception to Ni^{2+} (Fig. 11). Previous report appeared that the addition of transition metal ions such as Fe^{3+} , Co^{2+} , Zn^{2+} and Cu^{2+} inhibited the activity of the GDSL through conformational changes of the enzyme.^[20,42] In contrast, additional Fe^{3+} , Co^{2+} , and Cu^{2+} on ITBGDSL_1 increased the activity, indicating that the conformation of the enzyme is preferable for its activity. In the presence of Ca^{2+} and Zn^{2+} ions, the activity of ITBGDSL_1 was increased. In contrast, the activity of some GDSL, such as the enzyme from *G.*

thermocatenulatus and *Ruminococcaceae bacterium*, was decreased. Ca^{2+} was proposed to stabilize tertiary structure of the enzyme.^[10,20,43] In some lipase Ca^{2+} ion appeared to have function as ligand, binds to amino acid residues at the active site, maintaining the structural stability of the enzyme. The loss of Ca^{2+} might affect disruption of the structure and reduce the stability.^[44]

The activity of ITBGDSL_1 was inhibited by the present of Ni^{2+} . Previous studies reported similar phenomenon.^[45,46] The inhibition might due to Ni^{2+} interact to the functional histidine residue at active site of the enzyme.^[46] Previous study reported that metal ions could form complexes with ionized fatty acids, altering their solubility and behaviour at interfaces.^[47] The release of fatty acids into the medium is a rate-determining factor and might be influenced by metalions.^[10] However, the effect of metal ions depends on the

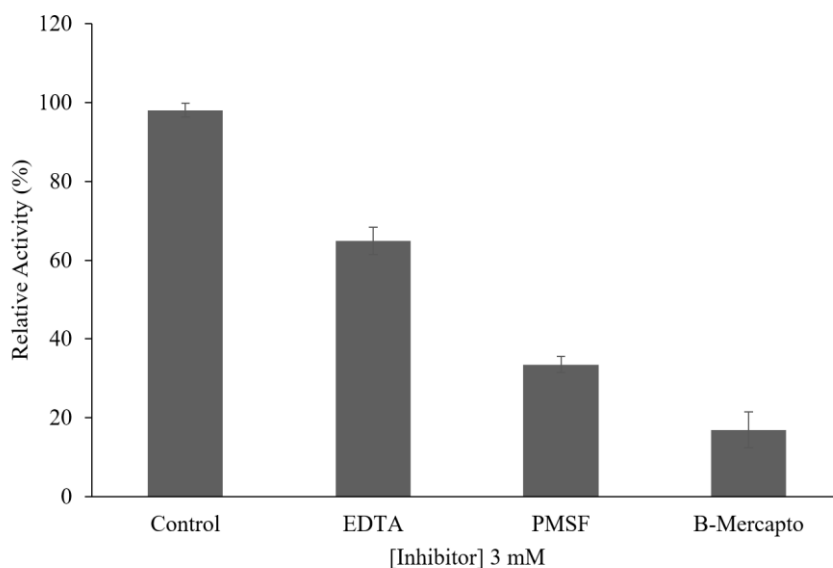


Fig. 10: Relative Activity of ITBGDSL_1 in the presence of variation inhibitor. (Control) Ethanol.

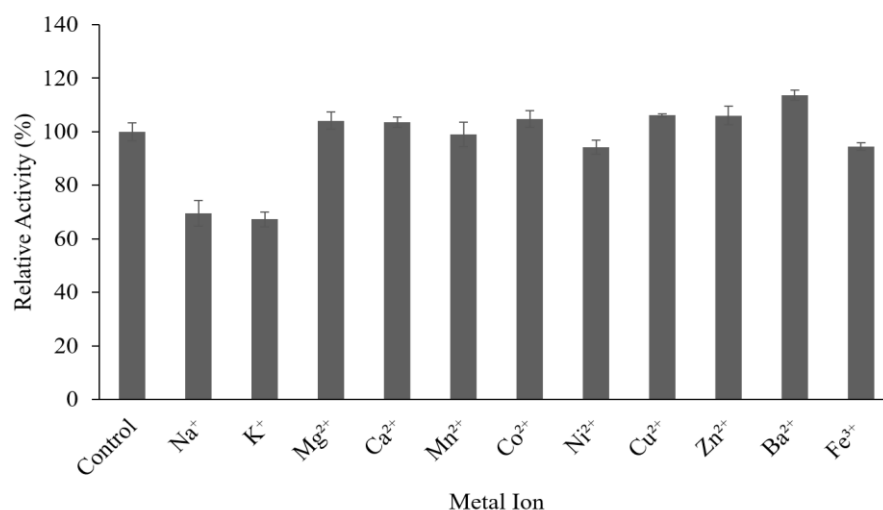


Fig. 11: Relative activity of ITBGDSL_1 on the present of metal ions (3 mM). Control reaction mixture without addition of metal ions.

structure and conformation of each enzyme.

Orientation of his loop at the active site of the enzyme (Fig. 12) is a critical factor for the interaction of the enzyme with the substrate. The distance between Ser10-His188 and His188-Asp185 on ITBGDSL_1 was influenced by the presence of metal ions (Table 7). In the presence of Cu²⁺ and Zn²⁺, the distance is closer, but the activity of the enzyme was increased. Meanwhile, in most of the characterised GDSL, such as MTG,^[36] Tlip,^[42] EstR5,^[20] and 643A,^[31] the presence

of Cu²⁺ and Zn²⁺ ions results in longer distances between Ser-His and decreases the activity of the enzymes (Table 8). The data support that the confirmation of his loop is a critical factor for the activity of the enzyme. However, the response of ITBGDSL_1 to the presence of a few metal ions was opposite to that of other GDSLs, suggesting that molecular interaction of catalytic process in ITBGDSL_1 is different from the others and hence ITBGDSL_1 might be a new member of the GDSL family and employ a different catalytic mechanism.

Table 7: The effect of metal ion on the distance of Ser-His and His-Asp at the catalytic pocket of ITBGDSL_1. The distance was calculated by PyMol software.

Enzyme	Metal Ion	Ser-His (Å)	His-Asp (Å)
ITBGDSL_1	None	3.2	3.1
	Mg ²⁺	3.0	2.4
	Co ²⁺	3.0	2.4
	Zn ²⁺	3.0	2.4
	Cu ²⁺	3.0	2.4

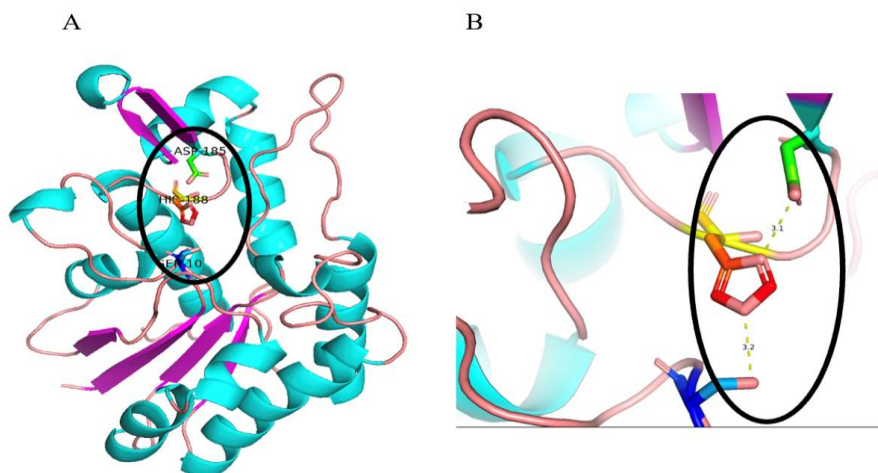


Fig. 12: 3D structure modelling of ITBGDSL_1 with the orientation of triad catalytic. (A) The whole enzyme; (B) Orientation of triad catalytic. (SER10) Serine; (ASP185) Aspartate; (HIS188) Histidine.

Table 8: The effect of Cu²⁺ and Zn²⁺ metal ions on the orientation of his loop and the activity of the enzyme.

Name Enzyme	Metal Ions								
	None			Cu ²⁺			Zn ²⁺		
	S10- H188 (Å)	H188- D185 (Å)	Activity (%)	S10- H188 (Å)	H188- D185 (Å)	Activity (%)	S10- H188 (Å)	H188- D185 (Å)	Activity (%)
ITBGDSL_1 (this study)	3.1	3.1	100	3.0	2.4	106	3.0	2.4	106
EstR5 [20]	3.2	3.0	100	3.2	4.1	28.9	3.2	4.1	76.4
643A [31]	8.7	2.5	100	11.3	2.5	24	11.3	2.5	0
MT6 [36]	2.6	3.2	100	3.6	3.2	36.04	3.6	3.2	39.90
Tlip [42]	3.2	3.2	100	4.2	4.3	18	4.2	4.3	50

4. Conclusion

ITBGDSL_1 was successfully expressed in *E. coli* BL21 (DE3) and characterised. Homological analysis revealed that the enzyme showed all conserved regions in GDSL enzymes despite low homology to other GDSL-characterised enzymes. The enzyme exhibited hydrolysis activity to *p*NP-ester with optimum activity at 55 °C, pH 8, and *p*NP C2 as a substrate. Hydrolysis activity of ITBGDSL_1 prefers more polar solvents and was inhibited by EDTA, PMSF, β -mercaptoethanol, and surfactant. Furthermore, the activity of the enzyme was stable following incubation at the optimum temperature up to 60 h. The activity was influenced in the presence of metal ions. Monovalent ions such as Na⁺ and K⁺ deactivated. Meanwhile, most of the divalent metal ions activated the enzyme. The response of ITBGDSL_1 in the presence of some metal ions was opposite to that of the other GDSLs, suggesting ITBGDSL_1 has unique and potential biocatalytic properties.

Acknowledgments

This work was supported by a grant from the SIMLITABMAS “Doctoral Dissertation Research” project program, Ministry of Education, Culture, Research and Technology, Contract No. 036/E5/PG.02.00.PL/2024 and National Research and Innovation Agency, Contract No. 5/IV/KS/05/2023 and 333/ITI.B07/KS.00/2023.

Conflict of Interest

There is no conflict of interest.

Supporting Information

Applicable.

References

[1] Z. Yang, Y. Zhang, T. Shen, Y. Xie, Y. Mao, C. Ji, Cloning, expression and biochemical characterization of a novel, moderately thermostable GDSL family esterase from *Geobacillus thermodenitrificans* T2, *Journal of Bioscience and*

Bioengineering, 2013, **115**, 133-137, doi: 10.1016/j.jbiosc.2012.08.016.

[2] O. Alalouf, Y. Balazs, M. Volkinshtein, Y. Grimpel, G. Shoham, Y. Shoham, A new family of carbohydrate esterases is represented by a GDSL hydrolase/acetylxylylan esterase from *geobacillus stearothermophilus*, *Journal of Biological Chemistry*, 2011, **286**, 41993-42001, doi: 10.1074/jbc.M111.301051.

[3] Y. Okamura, T. Kimura, H. Yokouchi, M. Meneses-Osorio, M. Katoh, T. Matsunaga, H. Takeyama, Isolation and characterization of a GDSL esterase from the metagenome of a marine sponge-associated bacteria, *Marine Biotechnology*, 2010, **12**, 395-402, doi: 10.1007/s10126-009-9226-x.

[4] C. Upton, J. T. Buckley, A new family of lipolytic enzymes? *Trends in Biochemical Sciences*, 1995, **20**, 178-179, doi: 10.1016/s0968-0004(00)89002-7.

[5] L. Ding, M. Li, W. Wang, J. Cao, Z. Wang, K. Zhu, Y. Yang, Y. Li, X. Tan, Advances in plant GDSL lipases: from sequences to functional mechanisms, *Acta Physiologiae Plantarum*, 2019, **41**, 151, doi: 10.1007/s11738-019-2944-4.

[6] A. Cenci, M. Concepción-Hernández, V. Guignon, G. Angenon, M. Rouard, Genome-wide classification and phylogenetic analyses of the GDSL-type esterase/lipase (GELP) family in flowering plants, *International Journal of Molecular Sciences*, 2022, **23**, 12114, doi: 10.3390/ijms232012114.

[7] M. Volokita, T. Rosilio-Brami, N. Rivkin, M. Zik, Combining comparative sequence and genomic data to ascertain phylogenetic relationships and explore the evolution of the large GDSL-lipase family in land plants, *Molecular Biology and Evolution*, 2011, **28**, 551-565, doi: 10.1093/molbev/msq226.

[8] G. Shen, W. Sun, Z. Chen, L. Shi, J. Hong, J. Shi, Plant GDSL esterases/lipases: evolutionary, physiological and molecular functions in plant development, *Plants*, 2022, **11**, 468, doi: 10.3390/plants11040468.

[9] C. Lai, L. Huang, L. O. Chen, M. Chan, J. Shaw, Genome-wide analysis of GDSL-type esterases/lipases in *Arabidopsis*, *Plant Molecular Biology*, 2017, **95**, 181-197, doi:

- 10.1007/s11103-017-0648-y.
- [10] E. Jo, J. Kim, A. Lee, K. Moon, J. Cha, Identification and characterization of a novel thermostable GDSL-type lipase from *Geobacillus thermocatenulatus*, *Journal of Microbiology and Biotechnology*, 2021, **31**, 483-491, doi: 10.4014/jmb.2012.12036.
- [11] B. P. Dalrymple, D. H. Cybinski, I. Layton, C. S. McSweeney, G. P. Xue, Y. J. Swadling, J. B. Lowry, Three *Neocallimastix patriciarum* esterases associated with the degradation of complex polysaccharides are members of a new family of hydrolases, *Microbiology*, 1997, **143**, 2605-2614, doi: 10.1099/00221287-143-8-2605.
- [12] J. Li, U. Derewenda, Z. Dauter, S. Smith, Z. S. Derewenda, Crystal structure of the *E. coli* thioesterase II, a homologue of the human NEF-binding enzyme, *Nature Structural and Molecular Biology*, 2000, **7**, 555-559. doi: 10.1038/76776.
- [13] A. Mølgaard, S. Kauppinen, S. Larsen, Rhamnogalacturonan acylesterase elucidates the structure and function of a new family of hydrolases, *Structure*, 2000, **8**, 373-383, doi: 10.1016/S0969-2126(00)00118-0.
- [14] C. C. Akoh, G. C. Lee, Y. C. Liaw, T. Huang, J. F. Shaw, GDSL family of serine esterases/lipases, *Progress in Lipid Research*, 2004, **43**, 534-552, doi: 10.1016/j.plipres.2004.09.002.
- [15] J. L. Arpigny, K. E. Jaeger, Bacterial lipolytic enzymes: classification and properties, *Biochemical Journal*, 1999, **343**, 177-183, doi: 10.1042/bj3430177.
- [16] T. Panda, B. S. Gowrishankar, Production and applications of esterases, *Applied Microbiology and Biotechnology*, 2005, **67**, 160-169, doi: 10.1007/s00253-004-1840-y.
- [17] Y. Lo, S. Lin, J. Shaw, Y. Liaw, Crystal structure of *Escherichia coli* thioesterase I/protease I/lysophospholipase L1: consensus sequence blocks constitute the catalytic center of SGNH-hydrolases through a conserved hydrogen bond network, *Journal of Molecular Biology*, 2003, **330**, 539-551, doi: 10.1016/S0022-2836(03)00637-5.
- [18] Y. J. Park, S. Y. Choi, H. B. Lee, A carboxylesterase from the thermoacidophilic archaeon *Sulfolobus solfataricus* P1: Purification, characterization, and expression, *Biochimica et Biophysica Acta (BBA)-General Subjects*, 2006, **1760**, 820-828, doi: 10.1016/j.bbagen.2006.01.009.
- [19] S. Yu, B. Zheng, X. Zhao, Y. Feng, Gene cloning and characterization of a novel thermophilic esterase from *Fervidobacterium nodosum* Rt17-B1, *Acta Biochimica et Biophysica Sinica*, 2010, **42**, 288-295, doi: 10.1093/abbs/gmq020.
- [20] G. Wang, K. Meng, H. Luo, Y. Wang, H. Huang, P. Shi, X. Pan, P. Yang, B. Yao, Molecular cloning and characterization of a novel SGNH arylesterase from the goat rumen contents, *Applied Microbiology and Biotechnology*, 2011, **91**, 1561-1570, doi: 10.1007/s00253-011-3289-0.
- [21] J. Ding, T. Yu, L. Liang, Z. Xie, Y. Yang, J. Zhou, B. Xu, J. Li, Z. Huang, Biochemical characterization of a GDSL-motif esterase from *Bacillus* sp. K91 with a new putative catalytic mechanism, *Journal of Microbiology and Biotechnology*, 2014, **24**, 1551-1558, doi: 10.4014/jmb.1406.06056.
- [22] T. Yu, J. Ding, Q. Zheng, N. Han, J. Yu, Y. Yang, J. Li, Y. Mu, Q. Wu, Z. Huang, Identification and characterization of a new alkaline SGNH hydrolase from a thermophilic bacterium *Bacillus* sp. K91, *Journal of Microbiology and Biotechnology*, 2016, **26**, 730-738, doi: 10.4014/jmb.1507.07101.
- [23] M. Wicka-Grochocka, H. Cieśliński, M. Wanarska, Cloning, expression in *Komagataella phaffii*, and biochemical characterization of recombinant sequence variants of *Pseudomonas* sp. S9 GDSL-esterase, *Acta Biochimica Polonica*, 2021, **67**, 411-417, doi: 10.18388/abp.2020_5730.
- [24] S. F. Syihab, F. M. Warganegara, Akhmaloka, Isolation, characterization, and identification of lipolytic thermophiles with methanol tolerance from domestic compost, *Journal of Pure and Applied Microbiology*, 2015, **9**, 385-390, doi: 10.22207/JPAM.13.4.32.
- [25] Y. Lee, J. C. Chen, J. F. Shaw, The thioesterase I of *Escherichia coli* has arylesterase activity and shows stereospecificity for protease substrates, *Biochemical and Biophysical Research Communications*, 1997, **231**, 452-456, doi: 10.1006/bbrc.1997.5797.
- [26] S. Kumar, G. Stecher, M. Li, C. Knyaz, K. Tamura, MEGA X: molecular evolutionary genetics analysis across computing platforms, *Molecular Biology and Evolution*, 2018, **35**, 1547-1549, doi: 10.1093/molbev/msy096.
- [27] M. Mirdita, K. Schütze, Y. Moriwaki, L. Heo, S. Ovchinnikov, M. Steinegger, ColabFold: making protein folding accessible to all, *Nature Methods*, 2022, **19**, 679-682, doi: 10.1038/s41592-022-01488-1.
- [28] W. L. DeLano, PyMOL: An open-source molecular graphics tool, *CCP4 Newsletter on Protein Crystallography*, 2002, **40**, 82-92.
- [29] O. Trott, A. J. Olson, AutoDock Vina: improving the speed and accuracy of docking with a new scoring function, efficient optimization, and multithreading, *Journal of Computational Chemistry*, 2010, **31**, 455-461, doi: 10.1002/jcc.21334.
- [30] M. H. Shakiba, M. S. M. Ali, Raja Noor Zaliha Raja Abd Rahman, A. B. Salleh, T. C. Leow, Cloning, expression and characterization of a novel cold-adapted GDSL family esterase from *Photobacterium* sp. strain J15, *Extremophiles*, 2016, **20**, 45-55, doi: 10.1007/s00792-015-0796-4.
- [31] H. Cieśliński, A. M. Białkowska, A. Długołęcka, M. Daroch, K. L. Tkaczuk, H. Kalinowska, J. Kur, M. Turkiewicz, A cold-adapted esterase from psychrotrophic *Pseudoalteromonas* sp. strain 643A, *Archives of Microbiology*, 2007, **188**, 27-36, doi: 10.1007/s00203-007-0220-2.

- [32] M. Barros, L. F. Fleuri, G. A. Macedo, Seed lipases: sources, applications and properties - a review, *Brazilian Journal of Chemical Engineering*, 2010, **27**, 15-29, doi: 10.1590/s0104-66322010000100002.
- [33] Y. Kojima, M. Kobayashi, S. Shimizu, A novel lipase from *Pseudomonas fluorescens* HU380: gene cloning, overproduction, renaturation-activation, two-step purification, and characterization, *Journal of Bioscience and Bioengineering*, 2003, **96**, 242-249, doi: 10.1016/S1389-1723(03)80188-3.
- [34] C. D. Anobom, A. S. Pinheiro, R. A. De-Andrade, E. C. G. Aguiaras, G. C. Andrade, M. V. Moura, R. V. Almeida, D. M. Freire, From structure to catalysis: recent developments in the biotechnological applications of lipases, *BioMed Research International*, 2014, **2014**, 684506, doi: 10.1155/2014/684506.
- [35] T. Furqan, S. Batool, R. Habib, M. Shah, H. Kalasz, F. Darvas, K. Kuca, E. Nepovimova, S. Batool, S. M. Nurulain, Cannabis constituents and acetylcholinesterase interaction: molecular docking, *in vitro* studies and association with *CNR1* rs 806368 and *ACHE* rs17228602, *Biomolecules*, 2020, **10**, 758, doi: 10.3390/biom10050758.
- [36] D. Deng, Y. Zhang, A. Sun, J. Liang, Y. Hu, Functional characterization of a novel marine microbial GDSL lipase and its utilization in the resolution of (\pm)-1-phenylethanol, *Applied Biochemistry and Biotechnology*, 2016, **179**, 75-93, doi: 10.1007/s12010-016-1980-4.
- [37] A. C. Dumetz, A. M. Chockla, E. W. Kaler, A. M. Lenhoff, Effects of pH on protein-protein interactions and implications for protein phase behavior, *Biochimica et Biophysica Acta (BBA) - Proteins and Proteomics*, 2008, **1784**, 600-610, doi: 10.1016/j.bbapap.2007.12.016.
- [38] T. R. Moharana, N. M. Rao, Substrate structure and computation guided engineering of a lipase for omega-3 fatty acid selectivity, *PLoS One*, 2020, **15**, e0231177, doi: 10.1371/journal.pone.0231177.
- [39] M. Miotto, P. P. Olimpieri, L. Di Rienzo, F. Ambrosetti, P. Corsi, R. Lepore, G. G. Tartaglia, E. Milanetti, Insights on protein thermal stability: a graph representation of molecular interactions, *Bioinformatics*, 2019, **35**, 2569-2577, doi: 10.1093/bioinformatics/bty1011.
- [40] B. Folch, M. Rooman, Y. Dehouck, Thermostability of salt bridges versus hydrophobic interactions in proteins probed by statistical potentials, *Journal of Chemical Information and Modeling*, 2008, **48**, 119-127, doi: 10.1021/ci700237g.
- [41] F. Kovacic, N. Babic, U. Krauss, K.-E. Jaeger, Classification of lipolytic enzymes from bacteria, *Aerobic Utilization of Hydrocarbons, Oils, and Lipids*, Cham: Springer International Publishing, 2019, 255-289, doi: 10.1007/978-3-319-50418-6_39.
- [42] N. Yu, J. Yang, G. Yin, R. Li, W. Zou, C. He, Identification and characterization of a novel esterase from *Thauera* sp, *Biotechnology and Applied Biochemistry*, 2018, **65**, 748-755, doi: 10.1002/bab.1659.
- [43] M. E. M. Noble, A. Cleasby, L. N. Johnson, M. R. Egmond, L. G. J. Frenken, The crystal structure of triacylglycerol lipase from *Pseudomonas glumae* reveals a partially redundant catalytic aspartate, *FEBS Letters*, 1993, **331**, 123-128, doi: 10.1016/0014-5793(93)80310-q.
- [44] J. F. A. Simons, M. D. van Kampen, I. Ubarretxena-Belandia, R. C. Cox, C. M. Alves dos Santos, M. R. Egmond, H. M. Verheij, Identification of a calcium binding site in *Staphylococcus hyicus* lipase: generation of calcium-independent variants, *Biochemistry*, 1999, **38**, 2-10, doi: 10.1021/bi981869l.
- [45] E. S. Al-Farraj, A. M. Younis, G. M. A. El-Reash, Synthesis, characterization, biological potency, and molecular docking of Co^{2+} , Ni^{2+} and Cu^{2+} complexes of a benzoyl isothiocyanate based ligand, *Scientific Reports*, 2024, **14**, 10032, doi: 10.1038/s41598-024-58108-5.
- [46] L. Xie, R. Liu, X. Chen, M. He, Y. Zhang, S. Chen, Micelles based on lysine, histidine, or arginine: designing structures for enhanced drug delivery, *Frontiers in Bioengineering and Biotechnology*, 2021, **9**, 744657, doi: 10.3389/fbioe.2021.744657.
- [47] F. Hasan, A. Ali Shah, A. Hameed, Industrial applications of microbial lipases, *Enzyme and Microbial Technology*, 2006, **39**, 235-251, doi: 10.1016/j.enzmictec.2005.10.016.

Publisher's Note: Engineered Science Publisher remains neutral with regard to jurisdictional claims in published maps and institutional affiliations.

Open Access

This article is licensed under a Creative Commons Attribution 4.0 International License, which permits the use, sharing, adaptation, distribution and reproduction in any medium or format, as long as appropriate credit to the original author(s) and the source is given by providing a link to the Creative Commons License and changes need to be indicated if there are any. The images or other third-party material in this article are included in the article's Creative Commons License, unless indicated otherwise in a credit line to the material. If material is not included in the article's Creative Commons License and your intended use is not permitted by statutory regulation or exceeds the permitted use, you will need to obtain permission directly from the copyright holder. To view a copy of this License, visit <http://creativecommons.org/licenses/by/4.0/>.

©The Author(s) 2025